Science in China Ser. B Chemistry 2004 Vol.47 No.1 80—90

Spectroscopic evidence for triplet excitation energy transfer among carotenoids in the LH2 complex from photosynthetic bacterium *Rhodopseudomonas palustris*

FENG Juan[1], WANG Qian[2], ZHANG Xujia[2], HUANG Youguo[2], AI Xicheng[1], ZHANG Xingkang[1] & ZHANG Jianping[1]

1. State Key Laboratory for Structural Chemistry of Unstable and Stable Species, Institute of Chemistry, Chinese Academy of Sciences, Beijing 100080, China;
2. National Laboratory of Biomacromolecules, Institute of Biophysics, Chinese Academy of Sciences, Beijing 100101, China
Correspondence should be addressed to Zhang Jianping (email: jpzhang@mail.iccas.ac.cn)

Received September 8, 2003

Abstract The LH2 complex from *Rhodopsudomonas (Rps.) palustris* is unique in the heterogeneous carotenoid compositions. The dynamics of triplet excited state Carotenoids (^{3}Car*) has been investigated by means of sub-microsecond time-resolved absorption spectroscopy both at physiological temperature (295 K) and at cryogenic temperature (77 K). Broad and asymmetric $T_n \leftarrow T_1$ transient absorption was observed at room temperature following the photo-excitation of Car at 532 nm, which suggests the contribution from various carotenoid compositions having different numbers of conjugated C=C double bonds ($N_{C=C}$). The triplet absorption bands of different carotenoids, which superimposed at room temperature, could be clearly distinguished upon decreasing the temperature down to 77 K. At room temperature the shorter-wavelength side of the main $T_n \leftarrow T_1$ absorption band decayed rapidly to reach a spectral equilibration with a characteristic time constant of ~1 μs, the same spectral dynamics, however, was not observed at 77 K. The aforementioned spectral dynamics can be explained in terms of the triplet-excitation transfer among heterogeneous carotenoid compositions. Global spectral analysis was applied to the time-resolved spectra at room temperature, which revealed two spectral components peaked at 545 and 565 nm, and assignable to the $T_n \leftarrow T_1$ absorption of Cars with $N_{C=C}$=11 and $N_{C=C}$=13, respectively. Surprisingly, the decay time constant of a shorter-con- jugated Car, i.e. 0.72 μs (aerobic) and 1.36 μs (anaerobic), is smaller than that of a longer-con- jugated Car, i.e. 2.12 μs (aerobic) and 3.75 μs (anaerobic), which is contradictory to the general rule of carotenoids and relative polyenes. The results are explained in terms of triplet-excitation transfer among different types of Cars. It is postulated that two Cars with different conjugation lengths coexist in an α, β-subunit in the LH2 complex.

Keywords: purple photosynthetic bacteria, carotenoid, excited-state, time-resolved spectroscopy.

DOI: 10.1360/03yb0104

Carotenoids (Car) are known to play at least two major physiological roles in photosynthetic organisms. They absorb blue-green light as accessory light-harvesting pigments, and then transfer the singlet-excita-

tion energy to the adjacent bacteriolchlorophyll (BChl) molecules. Two channels, i.e. both from the optically-allowed second singlet-excited state (S_2) to the Q_x state of BChl and from the optically-forbidden first singlet-excited state (S_1) to the Q_y state of BChl, can be very efficient. On the other hand, for Cars with nine or more conjugated C=C double bonds, their triplet excited-state energies are below the energies of singlet oxygen and triplet excited-state BChls, therefore they can prevent the generation of singlet oxygen by quenching triplet excited-state BChl or scavenge harmful singlet oxygen directly. In addition to the unique excited-state properties of Car, pigment-protein surroundings can also exert a significant influence on the aforementioned physiological functions of Cars.

During the past two decades, important structural information has been acquired by means of high- resolution X-ray crystallography with high-quality three-dimensional crystals of the light-harvesting complexes II (LH2) from purple photosynthetic bacteria. In 1995, McDermott et al.[1] succeeded in determining a 0.25-nm crystallographic structure of the LH2 complex from *Rhodopseudomonas* (*Rps.*) *acidophila*. In 1996, Koepke et al.[2] obtained a 0.24-nm structure of the LH2 complex from *Rhodospirillum* (*Rs.*) *molischianum*. These results show that the fundamental structural unit of LH2 complexes is a heterodimer consisting of two small transmembrane α- and β-apoproteins, to which BChl molecules are bound by forming coordination and/or hydrogen bonds with specific amino acid residues, whereas Cars are mainly stabilized by the dispersive interaction with the aromatic rings of amino acids or pyrole rings of BChls. In addition, Sundström et al.[3] have recently found the existence of weak hydrogen bonds between Car and BChl molecules on the basis of *ab intio* calculations. These interactions make all-*trans* Cars in the light- harvesting complexes slightly twisted, resulting in a partially-allowed S_1 state and, as a result, better energy transfer efficiency from this state to BChls. In the LH2 complex from *Rs. molischianum*, the closest edge-to- edge distance between Car and BChl is ~0.35 nm. This together with the optimized relative molecular orientation facilitates the efficient BChl-to-Car triplet energy transfer. Unlike *Rps. acidophila* and *Rs. molischianum* whose LH2 complexes contain only one major type of Car, heterogeneous compositions of Car are found in the LH2 complexes from strains such as *Rps. palustris* and *Rubrivivax gelatinosus*, providing us with an opportunity to address and access a number of interesting problems, such as the number of Cars in an α,β-subunit and the interaction among Cars, as well as their physiological implications. From the above considerations, the LH2 complex from purple photosynthetic bacterium *Rps. palustris* was selected and studied in this paper. It is unique in the following two aspects: (i) Five major Cars with different numbers of conjugated double bonds ($N_{C=C}$) were identified as lycopene ($N_{C=C}$=11), rhodopin ($N_{C=C}$ = 11), rhodovibrin ($N_{C=C}$ = 12), anhydrorhodovibrin ($N_{C=C}$ = 12) and spirilloxanthin ($N_{C=C}$ = 13); (ii) Depending on the light intensity and culturing time, the LH2 complex from *Rps. palustris* can be categorized into three different "spectral forms", i.e. the low-light form (LL) grown under a photon flux of ~100 lux, the intermediate-light form (ML) under ~1000 lux, and the high-light form (HL) under ~7000 lux. These spectral forms are distinguishable in terms of the stoichiometry ratio of pigments as well as the protein expression. Up to now, the LH2 complex from *Rps. palustris* has attracted intensive research interests largely owing to the unique spectroscopic properties of B800 BChl, a group of BChl molecules absorbing at ~ 800 nm. Various means had been employed including CD, LD, polarization fluorescence[4], time-resolved fluorescence spectroscopy[5] and resonance Raman spectroscopy[6]. As for the arrangement of Car molecules in this LH2 complex, however, no detailed structural information has been available. Although a satisfactory answer awaits a high-resolution crystallographic structure of the LH2 complex, spectroscopic methods are essential and useful to provide valuable structural information at the present stage.

The present paper reports the results of the LH2 complex obtained by the use of sub-microsecond time-resolved absorption spectroscopy both at room temperature (295 K) and at cryogenic temperature (77 K). Triplet excitation energy transfer among Cars with

different conjugated lengths was found at room temperature, and the rate significantly decreased upon decreasing the temperature down to 77 K. It is proposed that two Cars of different conjugation lengths coexist in an α,β-subunit in the LH2 complex from *Rps. palustris*, both of which keep close contact with BChl molecules.

1 Materials and methods

1.1 Isolation and purification of the LH2 complex

Cells of *Rps. palustris* were grown photoheterotrophically in Bose media[7] at a light intensity of ~4000 lux at 28℃ for about 50 h. The intermediate-light adapted LH2 complex (ML-LH2) was isolated and purified basically following the method described by Evans et al.[8] with certain modification. The cells harvested were sonicated at 4℃ (Cole parmer Ultrasonic homogenizer CPX 600) and digested by lysozyme (1 mg/mL) for 1 h, and the pellets (membranes) were precipitated by centrifugation at 150000×g for 1 h at 4℃ and re-suspended in 20 mmol/L Tris-HCl (pH 8.0) to give an absorption maximum of 50 cm^{-1} at 870 nm. The membranes were further solubilized with 1% (volume percent) lauryldimethylamine N-oxide (LDAO) and centrifuged at 5000×g for 10 min to remove the un-solubi- lized debris. The supernatant was diluted with 20 mmol/L Tris-HCl (pH 8.0) to bring the LDAO concentration to 0.3% (volume percent) and layered onto a sucrose step gradients consisting of 0.3, 0.6 and 1.2 mol/L sucrose in 20 mmol/L Tris-HCl (pH 8.0) and 0.1% (volume percent) LDAO. The gradients were centrifuged at 150000×g for 16 h at 4℃ and the protein band located between 0.3 and 0.6 mol/L sucrose was collected and dialyzed against the buffer containing 20 mmol/L Tris-HCl (pH 8.0) and 0.1% LDAO. The purity of the ML-LH2 complexes was >95% as estimated by the use of absorption spectrum and SDS-PAGE.

1.2 Sub-microsecond time-resolved spectroscopy

Fig. 1 shows the room-temperature absorption spectrum of the purified ML-LH2. Both peak wavelengths and relative heights of the absorption bands are in agreement with those reported in literatures[9]. For the measurements at cryogenic temperature (77 K), 60% glycerol (volume percent) was added to the suspension, and the mixture was frozen rapidly by the use of a cryostat (ST-100, Lauis Research Co., Inc.) to form a glassy block of optical quality. The optical path lengths are 5 and 2.5 mm for the room-temperature and the 77-K measurements, respectively. The optical density at the excitation wavelength of 532 nm was adjusted to 0.3—0.5 mJ per pulse. For the measurements at room temperature (295 K), oxygen was removed, when necessary, by adding 5 mmol/L glucose, 0.1 mg/mL glucose oxidase and 0.05 mg/mL catalase to the LH2 preparation, a method that was used in spectroscopic studies on photosystem II[10]. The sample cell was mounted on a translational stage to ensure that a fresh sample volume was exposed to each shot of pulsed excitation.

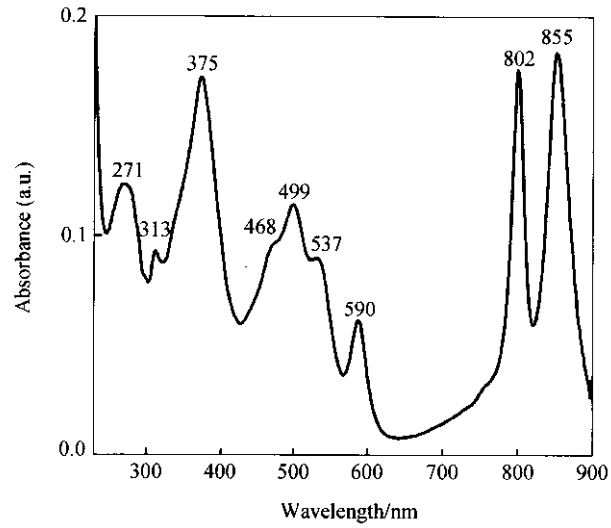

Fig. 1. Room-temperature absorption spectrum of the LH2 complex isolated from purple photosynthetic bacterium *Rps. palustris* in Tris-HCl (PH 8.0) buffer containing 0.1% LDAO.

The 532 nm excitation laser pulse (~ 10 ns, 10 Hz) was output from a Nd:YAG laser (571C, Quantel International). The excitation energy was attenuated to 2—3 mJ per pulse at the sample cell. White light pulses from a xenon flash lamp (L7685, Hamamatsu Photonics) were used as the probe. After passing the excited volume of sample the probe light was sent to a polychromator equipped with a gated linear photodi-

ode array detector (1420, EG&G; gate width 50 ns). An electric delay pulse generator (DG535, Stanford Research System) was used to regulate the delay time between the excitation and the gate pulses, the latter of which had been synchronized to the probe pulse. This apparatus allowed us to record transient spectra at selected delay times. Analysis on the time-resolved spectral data was carried out based on Matlab 5.2 (Mathworks) and Mathcad Pro7 (MathSoft).

2 Experimental results

2.1 Steady-state spectra

Fig. 1 shows typical room-temperature absorption spectrum of the LH2 complex isolated from *Rps. palustris* grown under the intermediate light. The strong absorption bands at 375 and 590 nm are ascribed to the Soret band and Q_x band of BChl, respectively, both of which exhibit only very small variations upon changing the environment. This is not the case for Q_y band, which undergoes a significant red-shift from 780 nm when BChl molecules are free in acetone, to 802 nm (denoted as B800) and 850 nm (denoted as B850) when they bind in the pigment-protein complex LH2. These significant shifts in absorption maxima mainly result from the formation of coordination bonds and hydrogen bonds with amino acids, as well as from the occurrence of strong interactions among BChls. The LH2 complex has its B850 absorption band lower than the B800 one, which is opposite to that seen in other strains of purple photosynthetic bacteria, such as *Rps. acidophila* and *Rs. molischianum*. This is not due to the low sample purity, and may arise from the following two reasons: (i) In contrast to other LH2 complexes which contain two B850 BChl and one B800 BChl molecules in an α,β-subunit, the 0.75-nm electron density map of the LH2 complex from *Rps. palustris* revealed the presence of an additional B800 BChl in an α, β-subunit[11]; (ii) The loss of hydrogen bonds, owing to the variation of the +13 and +14 amino acid in the α-apoprotein from Tyr and Trp to Phe and Met, results in a spectral blue-shift of the B850 absorption peak[12]. The above two factors should be responsible for the decease of the absorption ratio of B850/B800. More complicated situation is expected with regard to Cars because of spectral overlap from heterogeneous Cars compositions. As shown in fig. 1, three distinct absorption bands peaked at 468, 499 and 537 nm are related to $S_2 \leftarrow S_0$ transition. They can be attributed to the $0\leftarrow0$, $1\leftarrow0$ and $2\leftarrow0$ vibrational transitions despite the contribution from different Cars. Koyama et al.[13] have succeeded in isolating five different types of Cars, as those found in the LH2 from *Rps. palustris*, from the RC and LH1 complexes for *Rhodobium marinum*, and measured their steady- state absorption spectra in *n*-hexane. The energy level of the S_2 state exhibits a linear $1/(2N_{C=C}+1)$ dependence, and the molar extinction coefficient of the $S_2\leftarrow S_0$ absorption varies from one Car to another. With reference to literature results obtained under similar intermediate-light intensity[9], three major Cars in the LH2 complex of *Rps. palustris* are most likely to be spirilloxanthin (57%), rhodovibrin (20%) and lycopene (10%).

2.2 Time-resolved absorption spectra

Following the selective pulsed excitation of Car at 532 nm, a series of sub-microsecond time-resolved absorption spectra were recorded both at room temperature and at 77 K as presented in fig. 2(a)—(c). The time-dependent spectral changes are summarized as follows: (i) At 0.10 μs after the pulsed excitation, positive $T_n\leftarrow T_1$ absorption appeared at the longer-wavelength side of the negative ground-state bleaching signals (410—520 nm) both at room temperature ((a), (b)) and at 77 K (c). As the temperature decreased to 77 K, the main peak of $T_n\leftarrow T_1$ absorption experienced a spectral red-shift from 565 to 570 nm. Similarly, bleaching signals underwent a red-shift from 465 and 491 nm to 467 and 501 nm, respectively. The spectral shift mainly originated from the increase in the solvent density upon decreasing the temperature, which gave rise to higher optical refractive index and hence higher solvent polarizibility[14]. (ii) The room-temperature spectra revealed a weak shoulder (545 nm) located at the shorter-wavelength side of the main peak (565 nm), which decayed out completely within the delay time of 0.10—1.00 μs. This subtle change can be more clearly seen in fig. 3(a) and (b). Upon

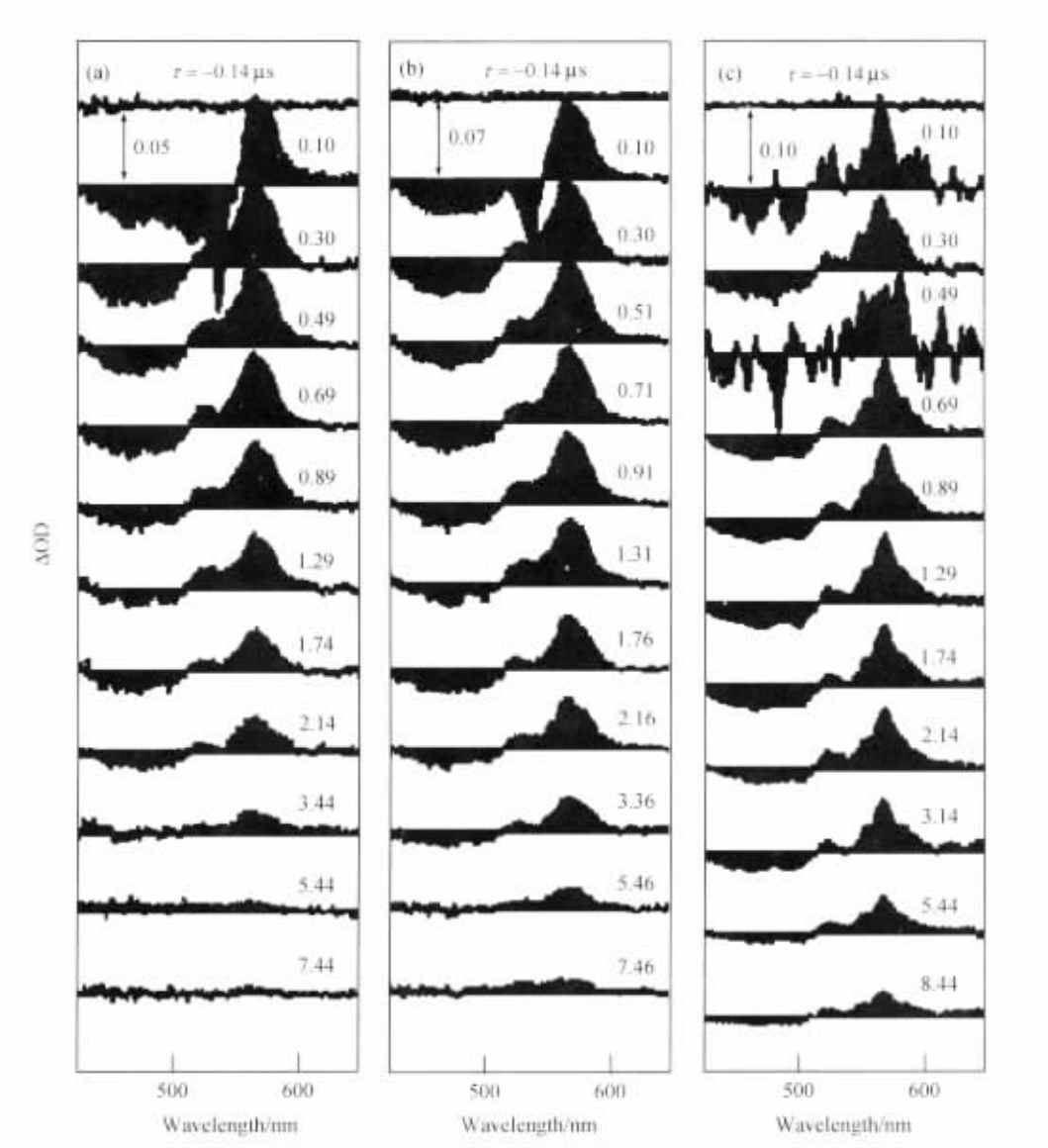

Fig. 2. Sub-microsecond time-resolved absorption spectra of carotenoids in the LH2 complex from *Rps. palustris* recorded following the pulsed excitation at 532 nm at room temperature under (a) aerobic and (b) anaerobic conditions, and (c) those recorded at 77 K. All the spectral curves are un-smoothed. The delay times between the probe and pump pulses as well as the scales of ΔOD are listed in each panel.

decreasing the temperature to 77 K, the shoulder peak, which shifted from 545 to 550 nm, can be distinguished from the main peak owing to the effect of spectral narrowing under cryogenic temperature. Here, it is interesting to address the following question, i.e. what is the reason of the broad and asymmetric overall $T_n \leftarrow T_1$ absorption at both room temperature and 77 K? Obviously, the absence of carboxyl group rules out the possibilities related to the breakdown in molecular symmetry or to the occurrence of intramolecular charge-transfer state in the Car molecules[15]. In view of the heterogeneous carotenoid compositions in the LH2 complex from *Rps. palustris*, we assign the broad and asymmetric features to the contributions from the triplet-excited states of different types of Cars generated under the pulsed excitation of Cars at 532 nm. (iii) The absorbance change of triplet-excited Car (ΔOD) reached a maximum at the delay time of 0.10

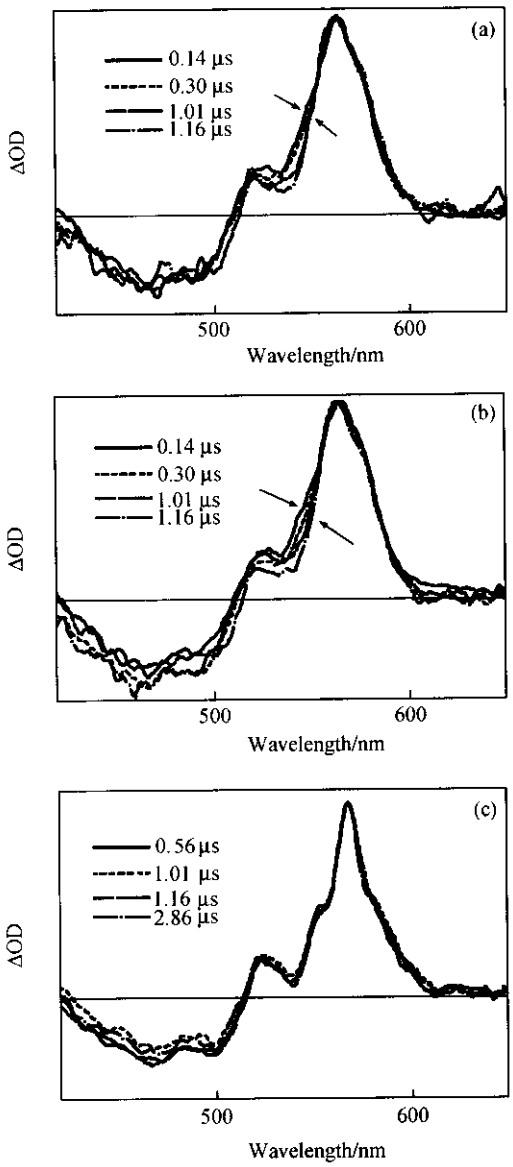

Fig. 3. Comparison of normalized $T_n \leftarrow T_1$ transient absorption spectra of the LH2 complex from *Rps. palustris* recorded at different delay times upon excitation at 532 nm at room temperature under (a) aerobic and (b) anaerobic condition, and (c) at 77 K. Spectral curves are appropriately smoothed.

μs at room temperature, indicating that the formation rate of $^3Car^*$ is faster than the instrumental response function (~50 ns). In the case of 77 K, however, a slow rising phase between 0.30 and 0.69 μs can be clearly identified from the time-evolution profiles monitored at 590 nm in fig. 4(d), though the transient spectra at the initial delay time (0.10—0.49 μs) were interfered by the 532 nm laser pulses. Similar phenomenon was observed with the pulsed excitation at 590 nm, corresponding to the Q_x absorption band of BChls (data not shown). The temperature-dependent building-up phase of $^3Car^*$ population is ascribed to the process of BChl-to-Car triplet energy transfer.

Generally speaking, a longer-conjugated Car has a lower triplet-excited state (T_1) and, as a result, a shorter T_1-state lifetime owing to the higher rate of intersystem crossing to the ground state[16]. However, our experimental results are in contradiction to the above general rules of carotenoids and relevant polyenes. As shown in fig. 3(a), in the delay time range of 0.00—0.16 μs, a shoulder peak appeared at 545 nm to the shorter-wavelength side of the main peak at 565 nm. Its relative intensity decreased as the delay time increased, and eventually vanished at 1.16 μs. As a result, the overall band width became narrower at the shorter-wavelength edge. However, the same type of spectra relaxation was not seen to the longer-wavelength side of the main $T_n \leftarrow T_1$ absorption band. This difference in spectral dynamics can be examined more clearly from the kinetics curves in fig. 4(a), where the triplet-excited Car at 545 nm decayed faster than the triplet-excited Car at 565 nm did. Thus a shorter-conjugated Car probed by the 545 nm trace had a shorter lifetime and a longer-conjugated Car probed at 565 nm had a longer lifetime, a fact which apparently deviates from the normal conjugation-length dependence of Car triplet lifetime. Similar results were observed under the anaerobic condition at room temperature, as evidenced in fig. 3(b) and fig. 4(b). The situation at 77 K is opposite to the case at room temperature, i.e. the distinct shoulder peak at 550 nm decayed slower than the main peak did. It is understandable that if there is no interaction or no energy transfer takes place among Cars, $^3Car^*$ would deactivate mainly via intersystem crossing to the ground state. The above experimental results suggested the presence of a temperature-dependent dynamic equilibrium among triplet-excited Cars (*vide infra*).

2.3 Global spectral analysis on the time-resolved absorption spectra

To obtain the $T_n \leftarrow T_1$ transient absorption spec-

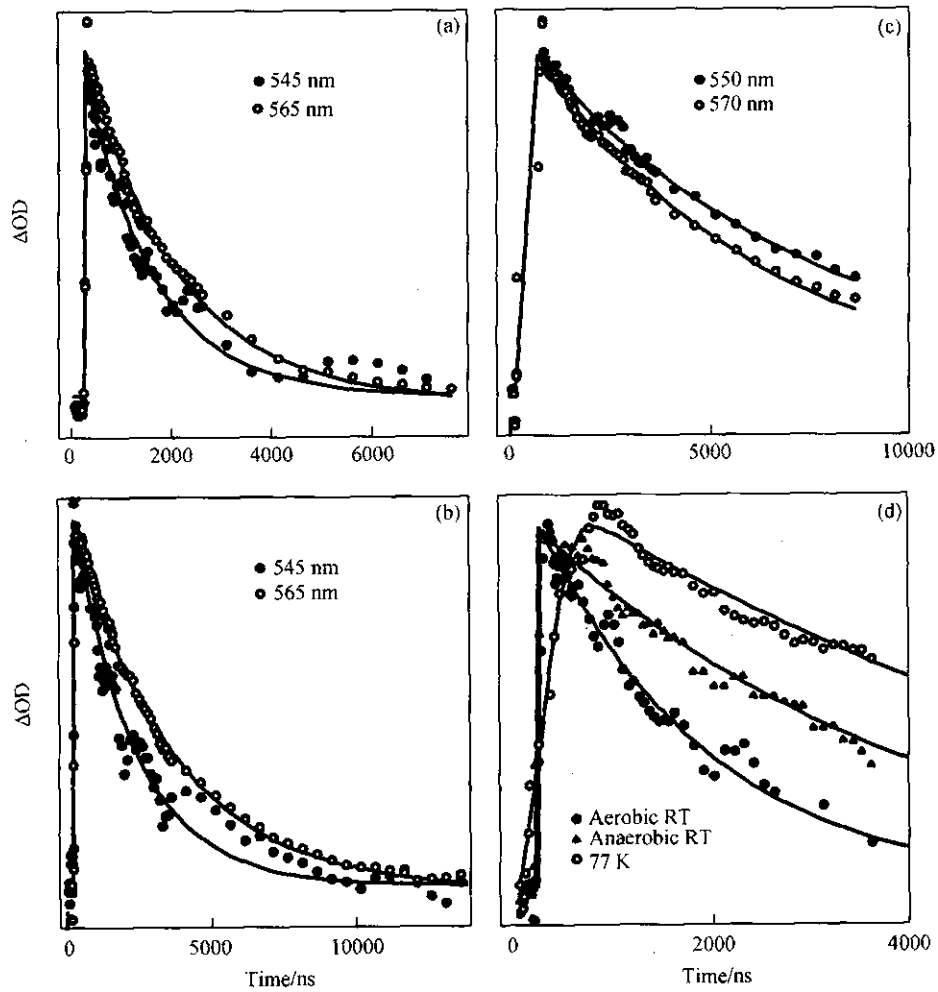

Fig. 4. Normalized kinetics traces plotted from the sets of time-resolved spectra of the LH2 complex from *Rps. palustris* as shown in fig. 2 at 545 nm (filled circle) and 565 nm (open circle) for (a) aerobic and (b) anaerobic cases, and at 550 nm (filled circle) and 570 nm (open circle) for the 77-K case (c). The temperature-dependent rising phase of $^3Car^*$ is clearly seen from the comparison of time-evolution profiles probed at 590 nm in fig. 4(d). Solid lines are fitting curves obtained from the global curve-fitting procedures.

trum associated with an individual Car, we had attempted singular value decomposition (denoted as SVD[17]) of the entire spectral data matrix typically consisting of 450 (wavelengths)×80 (delay times) data points. The SVD treatment yielded two significant singular values, i.e. S_{11} = 2.177 and S_{22} = 0.299, while the third one is relatively much weaker (S_{33} = 0.084). Because of the failure to reconstruct meaningful species associated difference spectra (SADS) and the time-evolution profiles owing to the poor signal-to- noise ratio of the time vectors, we then carried out general-purpose global curve fitting over twenty representative wavelengths from 460 to 605 nm. The room-temperature data under aerobic condition could be well accounted for by a summation of two exponential decays together with an addition increase component in the form of $1-\exp(-t/t)$. For the data under anaerobic condition a summation of three exponential decays was used to achieve a satisfactory fitting result. The 77 K-data could be fitted nicely by the use of two exponential decays. The SADS spectra and the corresponding time constants are depicted in fig. 5.

Global analysis yielded two main spectral com-

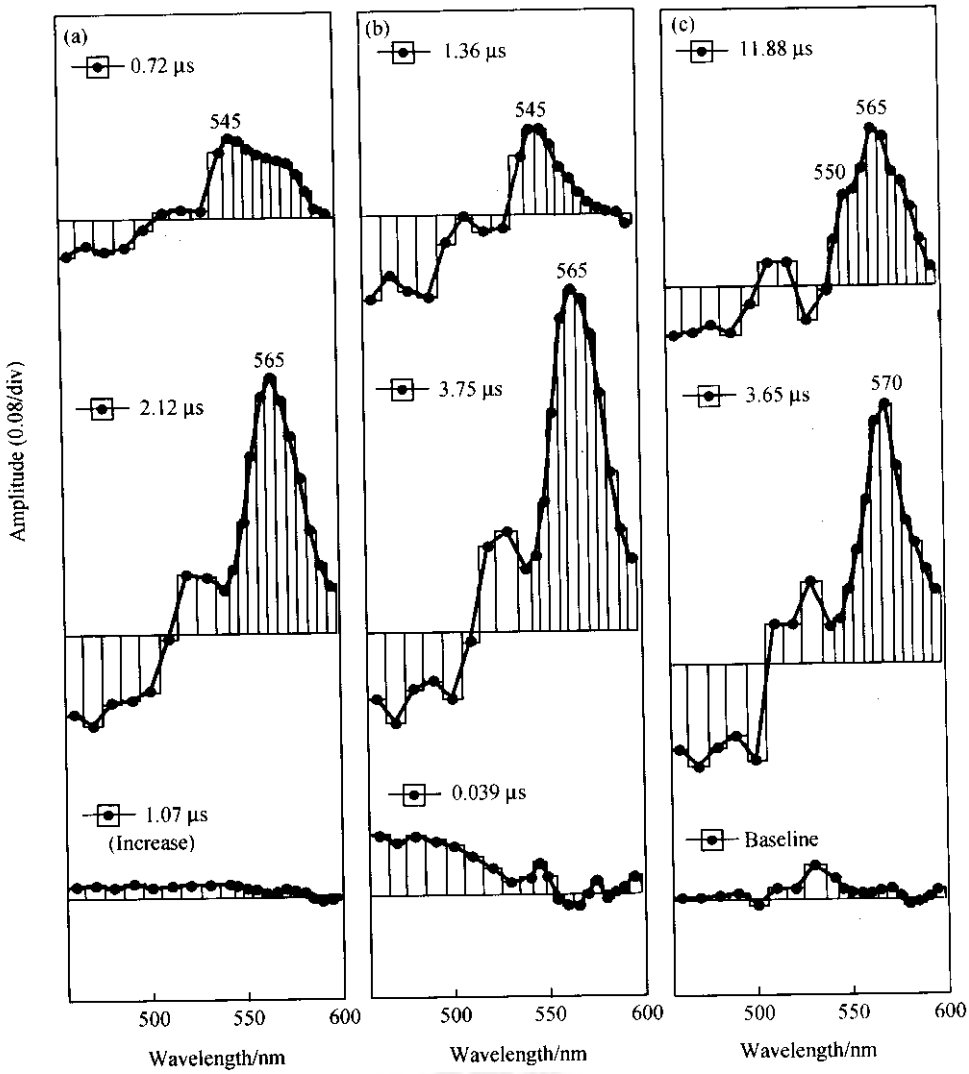

Fig. 5. SADS spectra and the associated time constants derived from the global spectral analysis on the time-resolved spectra of the LH2 complex from *Rps. palustris* as shown in fig. 2 (see text for details). Panels (a)—(c) correspond to those in fig. 2. The SADS spectra are listed in the order of Component-1, Component-2 and Component-3 from the top to the bottom in each panel.

ponents under aerobic condition at room temperature. Component-1 makes a contribution of ~25% in amplitude as measured at its peak wavelength of 545 nm, which can be ascribed to the $T_n \leftarrow T_1$ absorption originated from the group of Cars having eleven conjugated double bonds including lycopene and rhodopin. This assignment is based on the observation that lycopene and rhodopin glucoside in the LH2 complexes from *Rs. molischinanum* and *Rps. acidophila*, respectively, have the similar $T_n \leftarrow T_1$ transient energy[18]. One can easily recognize a 565 nm shoulder in the SADS spectra of Component-1, which is to be ascribed to Cars with longer-conjugated chain (*vide infra*). Component-2 contributes ~70% to the whole spectra with the absorption maximum at 565 nm. It was reported that $T_n \leftarrow T_1$ absorption of spirilloxanthin in cyclohexane is characterized by a transition energy of 560 nm[19]. Since the interaction with the protein environment may give rise to further spectral red-shift, we ascribe Component-2 to spirilloxanthin having thirteen conjugated double bonds. Component-3 is rather featureless and contributes only a few percent to the

whole $T_n \leftarrow T_1$ absorption spectra. This component increased in form of $1-\exp(-t/t)$ with a time constant of 1.07 μs. Further studies are necessary to clarify its origin.

Similar two spectral components were identified in the case of anaerobic treatment at room temperature. However, the triplet excited-state lifetimes of Component-1 and Component-2, 1.36 and 3.75 μs, respectively, both prolonged significantly with reference to those in the aerobic case (0.72 and 2.12 μs) mainly due to the weakening of spin-orbital coupling when the concentration of paramagnetic oxygen became much lower. In addition, the shoulder peak observed at 565 nm in Component-1 in the aerobic case was completely transferred to Component-2. Here again, Component-3, which lived shorter than the instrumental response time, provided only small contribution to the whole spectra. Regarding the negative feature seen at 560 nm in Component-3, it presumably reflects the formation phase of different types of Cars. In summary, the results obtained by the use of global analysis are in rough agreement with the original experimental data, i.e. the smaller the number of conjugated double bonds, the shorter the Car triplet-state lifetime, which is kinetically abnormal with reference to the aforementioned general rule of the conjugation-length dependence of T_1-state lifetime. For the measurement at 77 K, where 532 nm laser pulse exerts some influence on the rising phase of the $T_n \leftarrow T_1$ absorption spectra of $^3Car^*$ (fig. 2(c)), we made use of a bi-exponential function to fit the time-resolved spectra, and the result is shown in fig. 5(c). The peak wavelengths of $T_n \leftarrow T_1$ absorption of Component-1 experienced a 5 nm red-shift with respect to the corresponding room-temperature values. Different from the room-temperature cases, the absorption band at 565 nm became dominant in Component-1 at 77 K. This spectral component decayed with a time constant of 11.88 μs, and with a subtle shoulder band at 580 nm. Component-2 underwent a 5 nm red-shift to 570 nm with respect to the room temperature values, and made ~ 60% contribution to the overall $T_n \leftarrow T_1$ absorption. Its decay time constant is 3.65 μs. In comparison with the cases at room temperature, the triplet-state lifetime is significantly increased at 77 K mainly due to the reduction of radiationless relaxation process introduced by molecular vibrational motion. Most importantly, the lifetimes of triplet-state Car exhibited a normal conjugation-length dependence (*vide supra*) at 77 K, which is strikingly different from what observed at room temperature.

3 Discussion

Both the original time-resolved spectra (sec. 2.2) and the results of global analysis (sec. 2.3) indicate that $T_n \leftarrow T_1$ absorption spectra experienced a rapid dynamic equilibrium at physiological temperature. This process was observed either as a spectral narrowing, or as a faster decay of the shorter-conjugated Cars, both of which show a characteristic time constant of ~ 1.00 μs. Similar spectral dynamics was not observed in the 77-K measurements. The unique temperature-dependent spectral behavior is to be ascribed to triplet excitation transfer among different types of Cars.

In analogue to BChl-to-Car triplet energy, the Car-to-Car triplet excitation transfer is governed by Dexter's electron-exchange mechanism, which requires that energy donor and acceptor molecules must keep close proximity, for an instance, van der Waals contact, so as to achieve a reasonable overlap of electronic wavefunctions. To explain the abnormal spectral dynamics observed under room temperature, i.e. short-conjugated Cars have shorter apparent lifetimes, an assumption has to be made that the donor and the acceptor Car molecules having 11 and 13 conjugated double bonds, respectively, coexist in an α,β-subunit of the LH2 complex. In the 0.25-nm crystallographic structure of the LH2 from *Rps. acidophila*, the presence of a second Car molecule in an α,β-subunit was ambiguous, though one Car molecule in all-*trans* configuration has been clearly identified and found to make van der Waals contact with BChls[20]. A later spectroscopic study favored the coexistence of two Car molecules, whereas a careful stoichiometry study suggested only one[21]. Most recently, a 0.20-nm structure of the LH2 complex from *Rps. acidophila*

was determined, in which a second rhodopin glucoside molecule likely in a 12,15-*cis* configuration was found to keep van der Waals contact with both α- and β-B850s[22]. For the LH2 complex from *Rps. palustris*, on the other hand, no structural information on carotenoid molecules has been available. In the light of both spectroscopic and structural similarities between the LH2 complexes from *Rps. acidophila* and that from *Rps. palustris* grown under the intermediate light intensity, it is reasonable for us to make the above hypothesis of the coexistence of Cars.

As schematically displayed in fig. 6, triplet excitation transfer from Car1 to Car2 is energetically feasible. k_{ET} represents the rate of energy transfer, and k_{10} and k_{20} stand for the rate of intersystem crossing. We assume that Car1 and Car2 can be simultaneously excited ($N_1(t)$ and $N_2(t)$ represent the excited-state population; $N_1(t) = N_2(t) = 1$ at $t = 0$). Then Car population in the triplet-excited state can be expressed as

$$N_1(t) = \mathrm{e}^{-(k_{10}+k_{ET})t}, \tag{1}$$

$$N_2(t) = \frac{k_{ET}}{k_{20}-k_{10}-k_{ET}}(\mathrm{e}^{-(k_{10}+k_{ET})t} - \mathrm{e}^{-k_{20}t}) + \mathrm{e}^{-k_{20}t}. \tag{2}$$

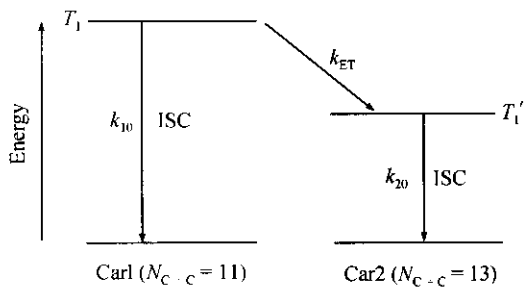

Fig. 6. A schematic presentation of triplet excitation transfer from Car1 to Car2.

Eq. (1) suggests that when $k_{ET} >> k_{10}$, ^{3}Car1* ($N_{C=C}$ =11) decays mainly via triplet energy transfer pathway with the time constant of k_{ET}, a situation which is in agreement with the results obtained at room temperature. Eq. (2) can be reorganized into

$$N_2(t) = A\mathrm{e}^{-(k_{10}+k_{ET})t} + B\mathrm{e}^{-k_{20}t}, \tag{3}$$

where $A = \dfrac{k_{ET}}{k_{20}-k_{10}-k_{ET}}$, and $B = \left(1 - \dfrac{k_{ET}}{k_{20}-k_{10}-k_{ET}}\right)$.

From eq. (3) it is clear that the population kinetics of Car2 ($N_{C=C}$ = 13) can be separated into two parts: One decays with the same time constant as Car1 does ($k_{10}+k_{ET}$), the other depends only on the intersystem-crossing rate of Car2 (k_{20}). The kinetics correlation explains why the SADS spectrum of Component-1 still contains the contribution from Component-2 (*vide supra*). In the case of 77 K where $k_{ET} < k_{10}$ and k_{20}, ^{3}Car1* and ^{3}Car2* relaxed back to the ground state mainly via intersystem crossing following the normal conjugation-length dependence of triplet-state lifetime. The slower rates observed at 77 K may partially originate from the spectral narrowing of both the phosphorescence emission spectrum of the donor Car1 and the phosphorescence excitation spectrum of the acceptor Car2, which would lead to a smaller spectral overlapping integral. We also need to consider another possible reason, i.e. the instantaneous fluctuation in molecular configuration and change in molecular position at 77 K can be frozen to a less extent with respect to the room-temperature cases. Since no apparent temperature-dependent term is in Dexter's original formulism, further theoretical studies are absolutely necessary to explain the temperature-dependence of the rate of triplet-energy transfer [18]. Nevertheless, our experimental results demonstrate that the triplet excitation transfer among Cars is a thermally-activated dynamic process, which is almost frozen out at 77 K.

5 Summary

We have concluded that the triplet excitation energy transfer among different types of Cars is responsible for the abnormal kinetics behavior of triplet excited-state Cars in the LH2 complex from *Rps. palustris*. Since the van der Waals contact between carotenoid molecules is a structural prerequisite for the triplet energy transfer to take place, there must be two different types of Cars in an α,β-subunit of the LH2 complex.

The coexistence of heterogeneous carotenoid compositions in the LH2 complex is expected to be of

physiological significance. On the one hand, Cars act as accessory light-harvesting pigments, on the other hand, they can effectively quench triplet-excited BChls, which otherwise would be a sensitizer for the generation of highly-reactive singlet-oxygen radical. It is well-known that shorter-conjugated Cars, for examples, spheroidene ($N_{C=C}$ = 10) and neurosporene ($N_{C=C}$ = 9) in *Rhodobacter (Rb.) sphaeroides* 2.4.1 and *Rb. sphaeroides* G1C, respectively, can trap light energy and transfer the singlet excitation to BChls with the efficiency as high as >90%. However, the five different types of Cars ($N_{C=C}$ =11—13) can only achieve 30%—40% Car-to-BChl singlet energy-transfer efficiency in the LH2 complex of *Rps. palustris*[9]. It seems that these longer-conjugated Cars mainly perform photoprotection function in the LH2 complex in question. The triplet excitation energy transfer mechanism proposed in the present paper implies that a unique photoprotection mechanism is developed in the LH2 complex of *Rps. palustris* cultivated under a higher light intensity.

Acknowledgements Zhang Jianping is indebted to the support from the Hundred-Talent Project of Chinese Academy of Sciences. This work was supported by the National Natural Science Foundation of China (Grant Nos. 20273077 and 39890390), and the State Key Basic Research and Development Plan (Grant No. G1998010100).

References

1. McDermott, G., Prince, S. M., Freer, A. A. et al., Crystal structure of an integral membrane light-harvesting complex from photosynthetic bacteria, Nature, 1995, 374: 517—521.
2. Koepke, J., Hu, X., Muenke, C. et al., The crystal structure of the light-harvesting complex II (B800-850) from *Rhodospirillum molischianum*, Structure, 1996, 4(5): 581—597.
3. He, Z., Sundström, V., Pullerits, T., Intermolecular hydrogen bonding between carotenoid and bacteriochlorophyll in LH2, FEBS Letters, 2001, 496: 36—39.
4. Moruik, F. V., Hawthornthwaitem, A. M., Vonk, C. et al., Spectroscopic characterization of the low-light B800-850 light-har- vesting complex of *Rhodopseudomonas Palustris*, strain 2.1.6, Biochim. Biophys. Acta, 1992, 1140: 85—93.
5. Nishimura, Y., Shimada, K., Yamazaki, I. et al., Energy transfer processes in *Rhodopseudomonas Palustris* grown under low-light conditions, FEBS Letters, 1993, 3 (29): 319—323.
6. Gall, A., Robert, B., Characterization of the different peripheral light-harvesting complexes from high- and low-light grown cells from *Rhodopseudomnononas Palustris*, Biochemistry, 1999, 38: 5181—5190.
7. Bose, S. K., Media for anaerobic growth of photosynthetic bacteria, in Bacterial Photosynthesis (eds. Gest, H., Pietro, A. S., Vernon, L. P.), Yellow Springs, OH: The Antioch Press, 1963.
8. Evans, M. B., Hawthornthwaite, A. M., Cogdell, R. J., Isolation and characterization of the different B800-850 light-harvesting complexes from low- and high-light grown cells of *Rhodopseudomonas Palustris*, strain 2.1.6, Biochim. Biophys. Acta, 1990, 1016: 71—76.
9. van Mourik, F., Hawthornthwaite, A. M., Vonk, C. et al., Spectroscopic characterization of the low-light B800-850 light-harvesting complex of *Rhodopseudomonas Palustris*, strain 2.1.6, Biochim. Biophys. Acta, 1992, 1140: 85—93.
10. Crystall, B., Booth, P. J., Klug, D. R. et al., Resolution of a long lived fluorescence component from D1/D2/cytochrome b-559 reaction centers, FEBS Letters, 1989, 249 (1): 75—78.
11. Hartigan, N., Tharia, H. A., Sweeney, F. et al., The 7.5-Å electron density and spectroscopic properties of a novel low-light B800 LH2 from *Rhodopseudomonas Palustris*, Biophys. J., 2002, 82 (2): 963—977.
12. Tharia, H. A., Hawthornthwaitem, T. D., Vonk, C. et al., Characterization of hydrophobic peptides by Rp-HPLC from different spectral forms of LH2 isolated from *Rps. Palustris*, Photosynthesis Research, 1999, 61: 157—167.
13. Qian, P., Saiki, K., Mizoguchi, T. et al., Time-dependent changes in the carotenoid composition and preferential binding of spirilloxanthin to the reaction center and anhydrorhodovibrin to the LH1 antenna complex in *Rhodobium marinum*, Photochemistry and Photobiology, 2001, 74 (3) : 444—452.
14. Frank, H. A., Joseu, J. S., Bautista, J. A. et al., Spectroscopic and photochemical properties of open-chain carotenoids, J. Phys. Chem. B, 2002, 106 (8): 2083—2092.
15. Frank, H. A., Bautista, J. A., Josue, J. et al., Effect of the solvent environment on the spectroscopic properties and dynamics of the lowest excited state of carotenoid, J. Phys. Chem. B, 2000, 104 (18): 4569—4577.
16. Burke, M., Land, E. J., McGarvey, D. J. et al., Carotenoid triplet state lifetimes, Journal of Photochemistry and Photobiology B: Biology, 2000, 59: 132—138.
17. Hofrichter, J., Henry, E. R., Sommer, J. H. et al., Nanosecond optical spectra of iron-cobalt hybrid hemoglobins: Geminate recombination, conformational changes, and intersubunit communication, Biochemistry, 1985, 24 (11): 2667—2679.
18. Bittl, R., Schlodder, E., Geisenheimer, I. et al., Transient EPR and absorption studies of carotenoids triplet formation in purple bacterial antenna complexes, J. Phys. Chem. B, 2001, 105(23): 5525—5535.
19. Rademaker, H., Hoff, A. J., Van Grondelle, R. et al., Carotenoid triplet yields in normal and deuterated *Rhodospirillum Rubrum*, Biochim. Biophys. Acta, 1980, 592 : 240—257.
20. Herek, J. L., Poĭvka, T., Pullerits, T. et al., Ultrafast carotenoid band shifts probe structure and dynamics in photosynthetic antenna complexes, Biochemistry, 1998, 37 (20): 7057—7061.
21. Arellano, J. B., Bangar Raju, B., Razi Naqvi, K. et al., Estimation of pigment stoichiometries in photosynthetic systems of purple bacteria: special reference to the (absence of) second carotenoid in LH2, Photochemistry and Photobiology, 1998, 68 (1): 84—87.
22. Papiz, M. Z., Prince, S. M., Howard, T. et al., The structure and thermal motion of the B800-850 LH2 complex from *Rps. acidophila* at 2.0 Å resolution and 100 K: New structural features and functionally relevant motions, J. Mol. Bio., 2003, 326: 1523—1538.